STRUCTURAL STUDIES OF CONTROLLED FE-C NANOCOMPOSITE SYSTEMS, GENERATED BY LASER PYROLYSIS

I. Morjan[1], F. Dumitrache[1], R. Alexandrescu[1], C. Fleaca[1], I. Sandu[1], I. Soare[1], I. Voicu[1], M. Savoiu[1], L. Albu[1], V. Ciupina[2], B. Rand[3],

[1]*National Institute for Lasers, Plasma and Radiation Physics, P.O. Box MG-36, 76900 Bucharest, Romania*

[2]*"Ovidius" University of Constanta,124 Mamaia Bd., P.O.B. 8600, Constanta, Romania*

[3]*Institute for Materials Research, School of Process, Environmental and Materials Engineering, University of Leeds, Leeds FS2 9TT, U.K.*

Corresponding author e-mail address:ralexa@ifin.nipne.ro

Abstract

The vapor-phase, laser-induced pyrolysis has been used to produce different iron-based nanoparticles coated by protective carbon layers. The synthesis process employs a CW CO_2 laser beam for continuously heating a gas mixture, in which iron pentacarbonyl (vapor) and acetylene/ethylene have been used as iron and carbon source, respectively. By well-controlled process conditions, homogeneously distributed particles (4-6nm average sizes) have been prepared. Changing the experimental parameters (e.g. laser power, reactor pressure), various structural features of the shell/core Fe/C nanoparticles may be evidenced. TEM, SAED, HRTEM investigations and Raman and FTIR techniques have been employed to characterize the nanocomposite systems.

Introduction

In the wide range of researches dedicated to nanostructured composites, the embedding of an inorganic core with either organic/carbonaceous [1-3] or inorganic [4] shell to form a core/shell (capsule-like) structure has lately attracted high interest. This shell-core structure is of considerable significance, not only because it offers an opportunity to investigate dimensionally confined systems, but also because the encapsulated species are likely to be immune to environmental effects or degradation, owing to the protective carbon shells around them [5]. Surface modifications that could bring novel physical and chemical properties to the nanostructured material are expected to open in many fields (magnetic, electronic, catalytic, biochemical) new important technological applications. Particularly attractive are magnetic embedded nanoparticles for magnetic recording, magnetic fluids and medicine. As potential candidates for ultrahigh density magnetic recording media of the next generation, size-controlled magnetic cores should be indispensable [6].

Metal nano-particles filled carbon nano-capsules have been produced by arc-discharge [7, 8], ion-beam sputtering methods [9], via solid-state reaction [5] and chemical

methods [6]. Of high interest is the study of the structural properties of these Fe/C nanocomposites since carbon may play an important role in the formation, structure and magnetic properties of nano-capsules [3]. More generally, many properties of nanoparticles especially those derived from their size-dependency may be generated by the synthesis method employed for their fabrication. Iron and iron oxide nanoparticles that present great interest due to their magnetic properties, have often been prepared either by using laser pyrolysis of iron pentacarbonyl ($Fe(CO)_5$) [10,11] or by using laser photolysis of ferrocene [12].

Recently we have reported the successful fabrication of carbon-encapsulated iron nanoparticles by laser pyrolysis from gas-phase precursors [13]. Direct evidence for the formation of the shell–core structure of Fe-C nanocomposites was revealed by using high-resolution transmission electron microscopy (HRTEM). The present work demonstrates that the laser pyrolysis process can produce shell/core Fe/C nanocomposites with various structural features and different mean particle diameters only by changing experimental parameters like laser power and reactor gas pressure. Particle sizes between 4 and 7 nm were obtained which increased with increasing the density of laser energy (i.e., increased induced reaction temperature). It was found that increasing the pressure is generating a higher order degree in the carbonaceous coverage of the iron cores.

Experimental

Core/shell Fe/C nanoparticles were prepared by the laser pyrolysis process as described in the previous work [13]. In the CO_2 laser synthesis method [14] the reactant gases are heated by laser absorption in a well-defined irradiated region. The process is based on the resonance between the laser radiation and a sensitizer. To synthesize Fe/C nanoparticles, iron pentacarbonyl ($Fe(CO)_5$) and acetylene (C_2H_2)/ ethylene (C_2H_4) were used as precursors. The focused continuous-wave CW CO_2 laser radiation (120 Watt maximum output power, λ = 10.6 μm) orthogonally crossed the gas flows emerging through three concentric nozzles. The reactant gases were confined to the flow axis by a coaxial Ar stream (outer tube). In order to prevent the NaCl windows from being coated with powder, they were continuously flushed with Ar. The interaction with the laser beam results in a bright flame. The nucleated particles formed in the reaction are entrained by the gas stream to the cell exit where they are collected on a microporous filter. The flow rates of the reactant mixture, of the sensitizer and of the Ar streams were independently controlled. During the experiment, liquid $Fe(CO)_5$ (about 25 torr vapor pressure at 20 ^{0}C) was bubbled with different C_2H_4 flow rates. Since the $Fe(CO)_5$ does not absorb in the 10 μm region, C_2H_4 was used as sensitizer (it is excited by the absorption of the CO_2 laser radiation and transfers, by collision the absorbed energy towards the other reaction partners, thus finally increasing the translation temperature of the whole system). Previous experiments have shown that $Fe(CO)_5$ decomposes and aggregates as iron clusters at relatively low temperatures (around 300 ^{0}C) for which ethylene remains stable. Nucleated particles formed during reaction are entrained by the flow to the cell exit into a trap, closed with a microporous filter in the direction of the rotary pump.

The morphology and composition of Fe-C nanocomposites were characterized by medium and high-resolution transmission electron microscopy (TEM and HRTEM), selected area electron diffraction (SAED), X-ray diffraction (XRD), Raman and FTIR spectroscopy. HRTEM and some TEM were performed on a FEI CM200F field emission TEM fitted with a Gatan Imaging Filter and operated at 200 kV; other TEM images were recorded on a TEM CM 120 Philips apparatus, acceleration voltage, 80 KV. The XRD diffractograms were obtained on a Siemens D 599 apparatus using the Cu K_α radiation. Raman spectra were performed using a Raman TM^{2001} apparatus, 785 nm wavelength in a 180° backscatter configuration and a 30 s integration time.

After synthesis, some of the as-prepared powders were toluene extracted using the Soxhlet method which enables a qualitative estimation of carbonaceous compounds involved as well as a residue free of many of the poly-aromatic hydrocarbons usually contained in a pyrolysis amorphous carbon. The toluene solution was filtered and the residue (toluene insoluble part) was dried and pressed in KBr pellets. The residue has then been analyzed by FTIR.

Results and Discussion

The scope of this paper is to study the structural features and the particle size distributions of the prepared Fe/C nanocomposite, as a function of some important experimental parameters like laser power and total pressure variation in the reactor. For some representative runs, the detailed conditions of the experiments discussed in this article are summarized in Table I. The C_2H_4 values for the mixture acetylene /ethylene (column 3) were kept constant. For the three samples labeled A, B, C, the laser power is continuously decreasing. In case of samples D and E, a higher reactor pressure was used for the synthesis of sample D relatively to E. Sample F was obtained at moderate reaction parameters (reactor pressure as well as carbonyl and acetylene flows) but at high laser power (85 W).

As already stressed in Ref. [13], we suppose that the nucleation in the gas phase of iron atoms is an essential step in a plausible scheme for the growth of carbon covered iron nanoparticles. It is obvious that the pyrolysis process was indirectly activated by the laser energy transfer from absorbing ethylene molecules to the other gas components. The thermodynamically favored process is the iron pentacarbonyl decomposition that first generates iron aggregates. The hydrocarbon decomposition is speeded up by the catalytic surface of freshly formed iron nanoparticles. Indeed, in the same laser-induced thermal conditions, the decomposition of ethylene-acetylene system does not occur.

Table 1. Experimental parameters* for some significant runs in the laser synthesis of carbon embedded iron nanoparticles.

Run	C2H4 ($Fe(CO)_5$ carrier) (sccm)	C_2H_4 (sccm)	C_2H_2 (sccm)	Laser power (W)	Pressure (mbar)
A	50	30	65	85	650
B	50	30	65	65	650
C	50	30	65	55	650
D	15	30	180	50	600
E	15	30	180	50	450
F	40	30	100	85	500

* During all experiments, the Ar flows for confinement and for windows cleaning were maintained at 1100 and 150 sccm, respectively.

The XRD patterns of the nanoparticles reveal the major presence of α- Fe and turbostratic C phases, regardless of the experimental parameters used. Such a typical spectrum is displayed in Figure 1 for sample B obtained at moderate laser intensities (see Table 1). The diffractogram evidences a broad peak centered on the 3.4 Å interplanar distance that could be ascribed to turbostratic-type carbon sheets [2, 15] forming the outside protective layers of the nanocapsules. The most intense peak centered on 2.02 Å may be attributed to bcc α-Fe (100) (100% relative intensity for d=2.027 Å). The rings corresponding to the bcc Fe were also observed in the SAED pattern (see below). However, it is worthwhile to note that the presence of Fe_3C carbide (d=2.014 Å) cannot be excluded. Much more, the broad feature of this peak could hinder other lower intensity Fe_3C lines (corresponding to diffraction planes (220), (102), (211) and (112)). On the other hand, iron carbides are known to possess a favored enthalpy of formation [1]. Due to the fact that in other regions of the spectrum Fe_3C lines (with 50% (rather high) relative intensities) –are not revealed it is suggested that the presence of Fe_3C is less probable. This statement is confirmed by selected area electron diffraction analysis of samples (see below the results of SAED analysis). Also interesting to note is that, in contrast to the information obtained by SAED technique, XRD analysis of composite samples does not reveal the presence of iron oxidized phases.

From the displayed HTREM image (Fig.2) obtained for sample A, the interlayer distances (110) for α-Fe (dark core) and (02) C for carbon sheets (surrounding stratified shells) could be identified. The particles are distinct one from another and the graphitic layers have an onion-like shape. An interface does not seem to exist between the core and the shell. The shell layers are characterized by curved lattice fringes of interplanar spacing 0.34 nm corresponding to the (002) lattice plane of graphite. This corresponds to the graphite-related peak at $2\theta = 26^{o}$ and suggests that these shells are graphitic carbon [2].

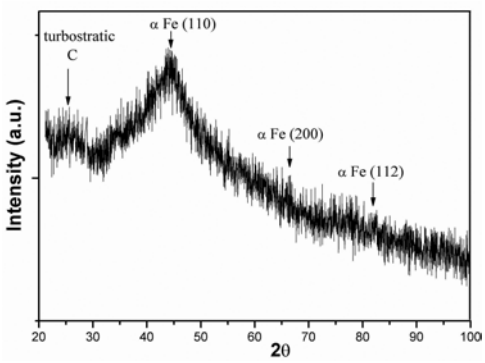

Figure 1. X-ray diffraction spectra of Fe-C nanocomposite powder.

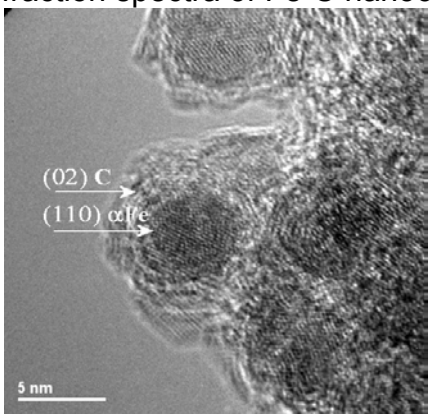

Figure 2. HRTEM images showing typical shell core structures of Fe/C nanoparticles (sample A)

The as prepared nanoparticles were toluene extracted. An enhanced high resolution image of particles is presented in Figure 3. Compared to non-treated samples, it is evident that the structure is different with a much thinner and uniform carbon shell (only 1-2 graphitic layers seem to surround the iron core). It is interesting to note that SAED determinations of the residue sample (not presented here) indicate the most intense ring at 2.03 Å which may be ascribed to (110) α-Fe. Also visible are rings at about 1.17 A ((211) α-Fe), 3.35 A ((200) graphitic carbon) and 2.52 ((311) gamma Fe_2O_3). It is worth noticing that in the sample residue after toluene extraction, the core-shell structure becomes better observable.

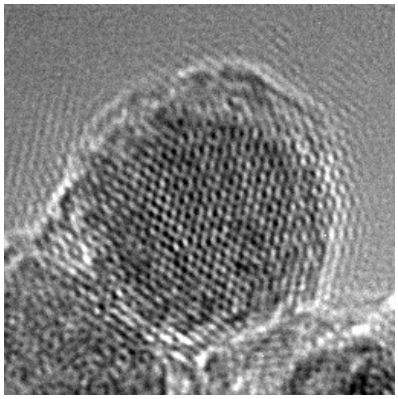
Figure 3. Enhanced HRTEM image of the residue resulted from toluene extraction.

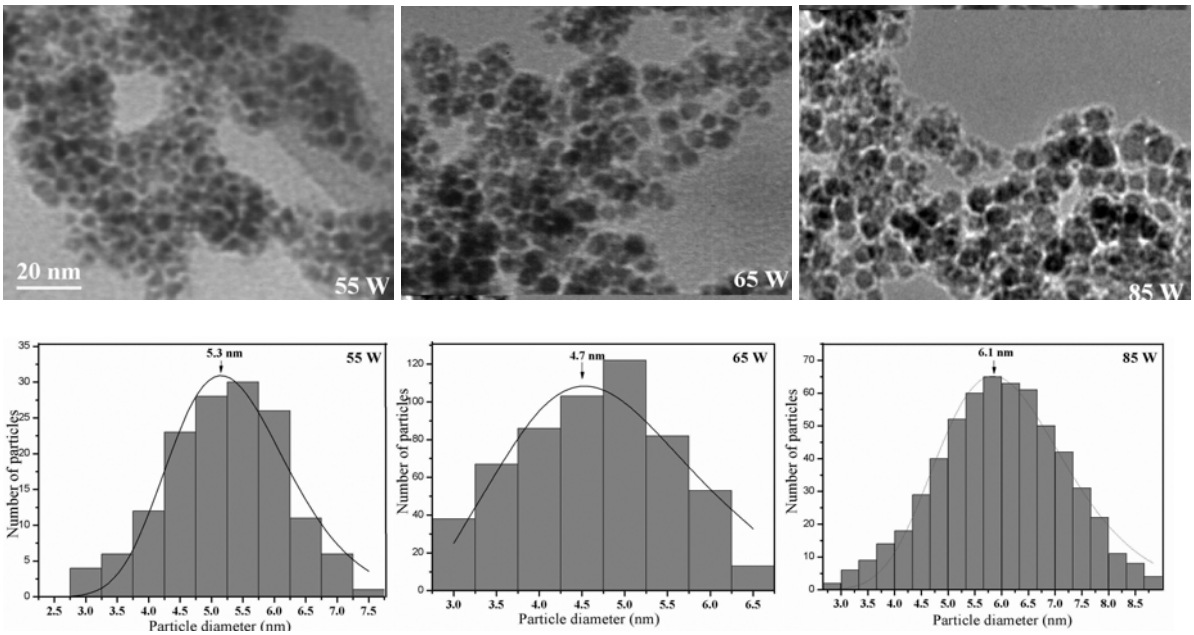

Figure 4. TEM images and corresponding particle size distributions for Fe/C samples obtained at increasing laser radiation intensity: 55 W (sample C), 65 W (sample B) and 85 W (sample A)

TEM images of Fe/C nanocomposite particles obtained at different intensities of the laser beam are exposed in Figure 4. For each of the three samples, the other synthesis parameters were maintained constant (see Table1). On the same Figure, the respective particle size distributions (calculated over more than 70 particles) are shown just beneath their own TEM images. In general, nanoparticles synthesized by this technique exhibit sharp particle size distributions, with low spreading of particle diameters around a mean value [13]. It is evident that increased laser beam intensity means an increased laser-induced reaction temperature in the absorbing gas-mixture. One may observe that at higher laser power (85 W for sample A) the particles seem to be rather distinct, presenting individualized structural features. The particle size distribution indicates a mean diameter around 6 nm. With decreasing laser power (65 W and 55 W for samples B and C, respectively), the tendency of inter-particle bridging appears (sample B) which becomes more pronounced and coalescent-like for sample C. However nanoparticle dispersion inside the carbon matrix seems to remain high. At the same time, there is a tendency of decreased mean diameter with decreasing laser power (around 5nm or even less - see Figure 4).

As shown in Figure 5, the selected area electron diffraction (SAED) pattern recorded from Fe/C nanoparticles reveals major bcc Fe phases (sample A). The SAED pattern of sample B is composed of an innermost diffraction ring corresponding to the graphite (002) spacing and of rings corresponding to the α-Fe phases. Complementarily, low oxidation features, representing the presence of the (311) γ-Fe_2O_3 and/or (121) Fe_3O_4 diffraction planes seem to be also present. For the particles coated incompletely by the

carbon shell, the oxides would exist in the surfaces of the particles [1]. The effect could be also correlated with iron nanoparticle decreasing size.

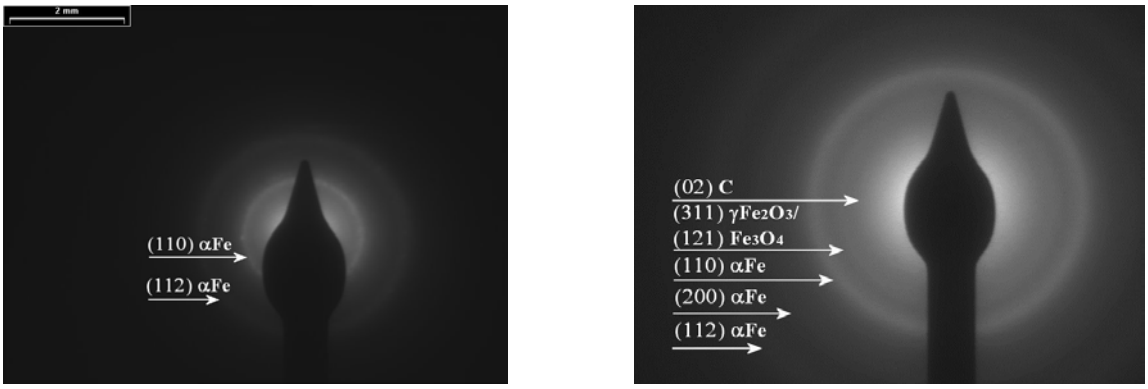

Figure 5. SAED patterns for Fe/C nanoparticles, sample A (on the left side) and sample B (on the right side).

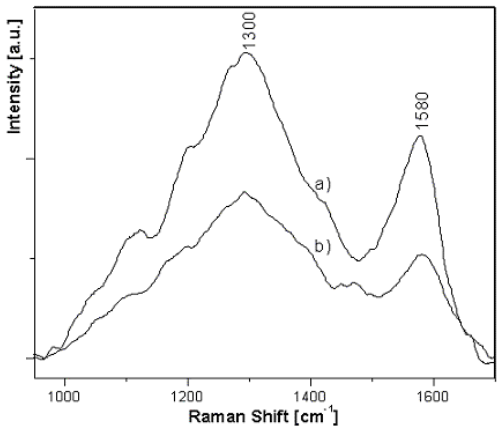

Figure 6. Raman spectra for two different Fe-C nanocomposite samples, obtained at two different reactor total pressures: a-sample D (650 mbar) and b-sample E (450 mbar)

Complementary information about the Fe-C nanocomposite structure was obtained from Raman investigation of samples. Figure 6 presents the Raman spectra of two samples obtained at two different reactor pressures, namely samples D (upper curve, 650 mbar) and E (lower curve, 450 mbar). We should note that in most laser pyrolysis experiments, increasing the pressure leads to enhanced reaction temperature due to the increased effect of the characteristic collisional energy transfer. In the carbon region of the spectrum, the D and G Raman bands appear well-defined and are centered on 1300 and 1580 cm^{-1}, respectively. However one could observe an increased sharpness of the G band with increasing pressure (i.e., increasing reaction temperature) that could signify an increased graphitization of the nanoparticle carbon shell. The sharp features of the G band seem to further increase by increasing the laser power (sample F in Figure 7). Figure 7 displays a comparison between the Raman spectra of the Fe/C nanocomposite (upper curve) and a nanocarbon sample (NC) obtained by laser pyrolysis from acetylene/ethylene precursors. NC sample was prepared with 500 W laser power, 750 mbar reactor pressure and a C_2H_2/C_2H_4 ratio equal to 5. It is known

that the two Raman features (G band of crystalline graphite and D band) could be a measure of the degree of order in an amorphous carbon sample. The ratio between intensities of D (1330 cm^{-1}) and G (1580 cm^{-1}) bands, I_D/I_G, correlates with the graphitic order, which could be characterized by the crystalline size L_a in the plane of graphene layers [17]. The calculated values of I_D/I_G, L_a, and band G width for Fe/C nanocomposite samples (E and D - obtained at different reactor pressures and F – at 85 W laser power) are compared in Table 2 with the same values of a nanocarbon sample (laser synthesized from the same hydrocarbon precursors). One observes that all L_a values for the Fe/C shell/core nanostructures are lower than that of nanocarbon sample, which could suggest a significant higher order degree in the carbon shell layers. An unusually low I_D/I_G ratio is found for sample F. An explanation for this behavior is not yet clear. It may be attributed to an increased order in the sp^2 domains of the carbon coverage. In [18], this effect is ascribed to the increase of sp^2 carbon relatively to sp^3.

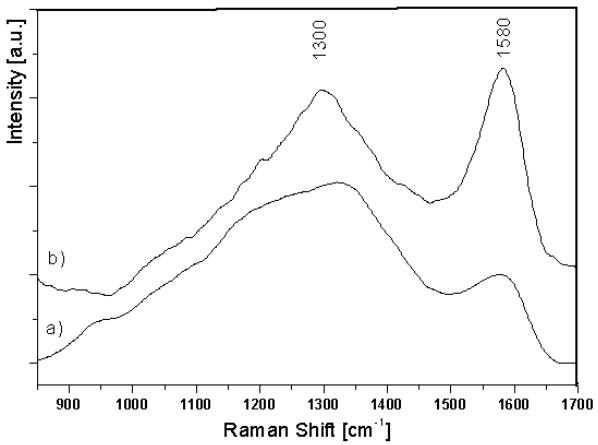

Figure 7. Comparison between the Raman spectra of Fe/C nanocomposites (sample F - curve a) and a nanocarbon sample issued by laser pyrolysing the same hydrocarbon precursors.

Table 2. The values of I_D/I_G, L_a, and band G width for Fe/C nanocomposite samples (obtained at different pressures and laser intensities) as compared with a nanocarbon (NC) sample (laser synthesized from the same hydrocarbon precursors)

Sample.	I_D/I_G	L_a [A]	Width (cm^{-1})
E	1.6	17.0	87.0
D	1.4	15.9	76.0
F	0.9	13.0	71.0
NC	2.0	20.7	64.0

The Fe/C shell/core nanostructures were examined by FTIR spectroscopy. In general, the samples exhibited similar spectral features. A typical example is presented in Figure 8 for sample F (curve a). In the 2000-3500 cm^{-1} spectral region, the spectrum appears as a triplet band located between 2850 and 3000 cm^{-1}. It may be ascribed to the CH

aliphatic stretch with its components at 2960 cm^{-1} (CH3 antisymmetric stretch), 2920 cm^{-1} (CH2 antisymmetric stretch), and 2850 cm^{-1} (CH2 symmetric stretch). The IR analysis of the sample residue (non-soluble components remained in the filter) is also presented in Figure 8 (curve b). As expected, in the 2000-3500 cm^{-1} region, the residue spectrum is exempt of any vibrations since the soluble carbonaceous components have not been retained by filtering.

Instead, significant (although with low intensity) transmission bands appear in the 400-700 cm^{-1} region which corresponds to the characteristic bands of iron oxides Some peaks are discerned in this large band (at about 625, 575, 528 and 480 cm^{-1}) which may be attributed to Fe_2O_3 or/and Fe_3O_4 and which seem to be enhanced in case of the toluene residue.

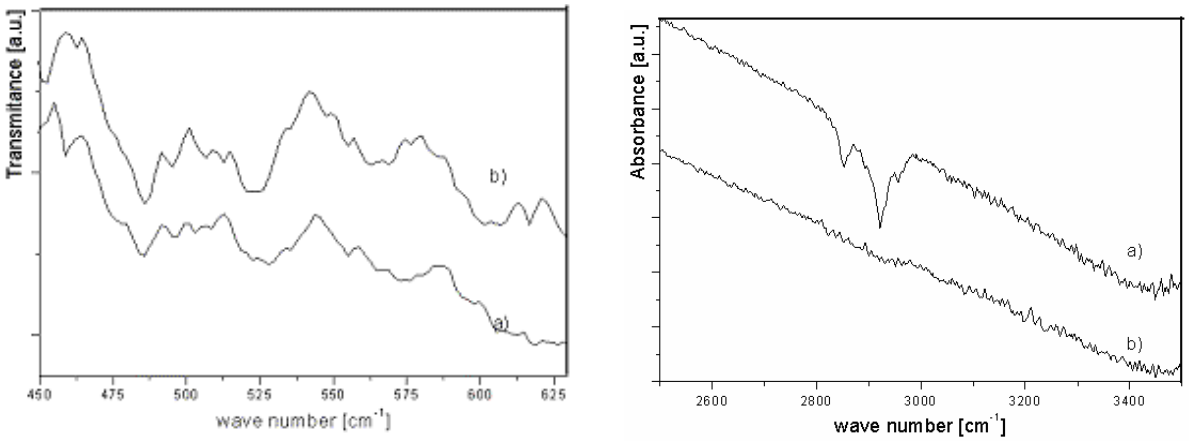

Figure 8. FTIR spectra of F Fe/C nanocomposite sample (a) and its residue (b) in the 400-700 cm^{-1} (left side) and 2000-3500 cm^{-1} (right side) wave-number regions. Spectrum (b) has been obtained from the dried residue of the toluene extract, i.e. from the nonsoluble part collected in the filter.

Conclusions

Carbon-coated iron nanoparticles have been synthesized from the gas phase, by using various experimental parameters in the laser pyrolysis process. The structural properties of the as-prepared shell/core Fe/C nanocomposite have been investigated by different analytical methods. A change in nanopowder morphology and a dependence of the particle mean size on different parameters (such as laser power and reactor total pressure) was established. Mean diameters between 4 and 7 nm and sharp particle distributions were found. The nano-cores seem to mainly consist of fcc iron with slight oxidation features (probably due to surface effects of incomplete coverage). No conclusive evidence of iron carbide formation was found. Important information about the carbon shell structure as derived from Raman analysis suggests that with increasing reaction temperature (laser power or/and reactor total pressure) there is an increase in the degree of graphitization of the carbon coverage.

Acknowledgements. The authors gratefully acknowledge the financial support from NATO SfP 974214 and the Romanian Ministry of Education and Research (Contract No. RO 90044)

References

[1] Wang ZH, Choi CJ, Kim BK, Kim JC, Zhang ZD. Characterization and magnetic properties of carbon-coated cobalt nanocapsules synthesized by the chemical vapor condensation process. Carbon 2003; 41:1751–1758

[2] Zhang ZD, Zheng JG, Skorvanek I, Wen GH, Kovac J, Wang FW, Yu JL, Li ZJ, Dong XL, Jin SR, Liu W, Zhang XX. Shell/core structure and magnetic properties of carbon-coated Fe–Co(C) nanocapsules. J. Phys.: Condens. Matter 2001;13:1921–1929.

[3] Dong XL, Zhang ZD, Chuang YC, Jin SR. Characterization of ultrafine Fe-Co particles and Fe-Co(C) nanocapsules. Phys. Rev. B 1999;60:3017-3020.

[4] Zeng Hao, Li Jing, Wang ZL, Liu JP, Sun Shouheng. Bimagnetic Core/Shell FePt/Fe_3O_4 Nanoparticles. Nanoletters 2004;4:187-190.

[5] Wu W, Zhu Z, Liu Z, Xie Y, Zhang J, Hu T. Preparation of carbon-encapsulated iron carbide nanoparticles by an explosion method. Carbon 2003;41: 317–321.

[6] Tomita S, Hikita M, Fujii M, Hayashi S, Yamamoto K. A new and simple method for thin graphitic coating of magnetic-metal nanoparticles. Chemical Physics Letters 2000;316:361–364.

[7] Chen CP, Chang TH, Wang TF. Synthesis of magnetic nano-composite particles. Ceramics International 2001;27:925–930.

[8] Saito Y. Nanoparticles and filled nanocapsules. Carbon 1995;33(7):979–988.

[9] Hayashji T, Hirono S, Tomita M, Umemura S. Magnetic thin films of cobalt nanocrystals encapsulated in graphite-like carbon. Nature 1996;381:772–774.

[10] Alexandrescu R, Cojocaru S, Crunteanu A, Morjan I, Voicu I, Diamandescu L, Vasiliu F, Huisken F, Kohn B. Preparation of iron carbide and iron nanoparticles by laser induced gas phase pyrolysis. J. Phys. IV France 1999;90:Pr8-537.

12. Xiang XB, Ganguly B, Huffman GP, Huggins FE, Endo M, Eklund PC. Nanocrystalline Alpha-Fe, Fe3c, and Fe7c3 Produced by Co2-Laser Pyrolysis. J. Mater. Res. 1993;8(7):1666.

[13] Elihn K, Otten F, Boman M, Heszler P, Kruis FE, Fissan H, Carlsson JO. Size distributions and synthesis of nanoparticles by photolytic dissociation of ferrocene. Appl. Phys. A 2001 ;72:29–34.

[14] Dumitrache F, Morjan I, Alexandrescu R, Morjan RE, Voicu I, Sandu I, Soare I, Ploscaru M, Fleaca C, Ciupina V, Prodan G, Rand B, Brydson R, Woodword A. Nearly monodispersed carbon coated iron nanoparticles for the catalytic growth of nanotubes/nanofibres. Diamond and Related Materials, 2003;13/2:362-370.

[15] Haggerty JS, Cannon WR. In Steinfeld JI editor. Laser induced chemical processes, vol. 165, New York; 1981.

[16] Wyckoff R.W.G. Crystal Structures, Wiley, New York, vol. 1:1963: 27-28.

[17] Ferrari AC, Robertson D. Multi-wavelength Raman spectroscopy of carbon. Phys Rev B 2000;61:14095.

[18] Chena JS, Laua SP, Chena GY, Suna Z, Lia YJ, Taya BK, Chaib JW, Diamond and Related Materials 2001;10:2018.